




RUBoost-Based Ensemble Machine Learning for Electrode Quality Classification in Li-ion Battery Manufacturing

Kailong Liu , Member, IEEE, Xiaosong Hu , Senior Member, IEEE, Jinhao Meng , Member, IEEE, Josep M. Guerrero , Fellow, IEEE, and Remus Teodorescu , Fellow, IEEE

I. INTRODUCTION

Abstract—As a typical mechatronics system, the battery manufacturing chain becomes a hot research topic because it directly determines electrode quality, further affecting manufactured battery performance. Due to the complexity of battery manufacturing, an effective sensitivity analysis solution that could quantify variable importance or correlations and explore impact variables toward resulting the electrode quality is urgently needed. This article scrutinizes the effects of component parameters from the mixing stage on the manufactured results of Li-ion battery electrode via classification modeling. Specifically, an effective RUBoost-based ensemble learning framework is proposed to compensate for class imbalance issue and well classify three key quality indicators including the electronic conductivity, thickness, and half-cell capacity for both LiFePO_4 - and $\text{Li}_4\text{Ti}_5\text{O}_{12}$ -based electrode. Experimental results reveal that the proposed models could well handle the class imbalance issues and accurately classify/predict the qualities of the manufactured electrode. Moreover, the importance weights of variables and the correlations of variable pairs could be effectively quantified. Due to the superiority in terms of accuracy, interpretability, and data-driven nature, the proposed ensemble learning approach could not only help to conduct reliable multiclassification of manufactured electrode but also benefit smarter battery manufacturing.

Index Terms—Li-ion battery, machine learning, quality prediction, smarter manufacturing, unbalanced classification.

Manuscript received 1 January 2021; revised 25 May 2021 and 9 August 2021; accepted 19 September 2021. Date of publication 18 October 2021; date of current version 17 October 2022. Recommended by Technical Editor Y. Liu and Senior Editor R. Gao. This work was supported in part by the National Natural Science Foundation of China under Grant 51875054, in part by the VILLUM FONDEN under the VILLUM Investigator Grant 25920, and in part by the China Postdoctoral Science Foundation under Grant 2020M673218. (Corresponding authors: Xiaosong Hu; Jinhao Meng.)

Warwick Manufacturing Group, University of Warwick, Coventry CV4 7AL, U.K. (e-mail: klu02@qub.ac.uk).

Department of Automotive Engineering, Chongqing University, Chongqing 400044, China (e-mail: xiaosonghu@ieee.org).

College of Electrical Engineering, Sichuan University, Chengdu 610065, China (e-mail: scmjh2008@163.com).

Center for Research on Microgrids (CROM), AAU Energy, Aalborg University, 9220 Aalborg, Denmark (e-mail: joz@et.aau.dk).

Department of Energy Technology, Aalborg University, 9220 Aalborg, Denmark (e-mail: ret@et.aau.dk).

Color versions of one or more figures in this article are available at <https://doi.org/10.1109/TMECH.2021.3115997>.

Digital Object Identifier 10.1109/TMECH.2021.3115997

LITHIUM-ION (Li-ion) battery represents one of the promising energy storage solutions for many applications such as electrical vehicle, owing to its high energy density, reliable service life [1], etc. However, the wider applications of Li-ion batteries are limited by their cost, reliability, safety, energy density, and life. As a typical mechatronics system, the battery production chain plays a vital and direct role in affecting the qualities of intermediate products, which, in turn, further determines final battery performance [2]. Therefore, it is crucial to monitor and analyze battery intermediate manufacturing processes in the pursuit of a smarter manufacturing chain [3], [4].

In general, battery manufacturing consists of three main processes including electrode production, battery assembly, and battery finishing. The electrode production process can be further divided into several individual steps such as mixing, coating, drying, calendaring, and cutting. As a highly complex process involving electrical, mechanical, and chemical engineering, the whole battery electrode production chain would generate a huge number of parameters in the order of tens or hundreds [3]. Understanding the individual or combined effects of these parameters on the manufactured electrode qualities is of extreme importance to optimize and improve the entire performance of the battery manufacturing chain. However, due to the complicated and strong-coupled characteristics of battery electrode production, the current mainstream solutions to analyze correlations among different parameters and further explore impact variables toward resulting manufactured electrode are still mainly based on the trial and error approaches, which is laborious and time-consuming. In this context, designing an effective artificial intelligence strategy to conduct reliable sensitivity analysis of parameters and predict the manufacturing quality is urgently needed.

With the rapid developments of cloud platform and artificial intelligence, data-driven solutions become one of the research hotspots in the field of mechatronics system [5], [6]. For battery applications, numerous machine learning technologies have been successfully derived to monitor battery internal states [7], predict battery lifetime [8], diagnose faults [9], achieve reliable charging control [10], [11], and energy management [12], [13]. All in all, through well designing suitable data-driven

approaches, effective improvement can be obtained for better battery management. However, these approaches mainly focus on the final battery properties without taking the qualities of the intermediate product (i.e., electrode) into account.

In comparison with the battery management area with fruitful solutions, fewer works have been done so far on adopting powerful machine-learning strategies to analyze battery productions. Among limited literature on battery manufacturing (e.g., adjustments [14] and monitoring [15]), a suitable data-driven approach to analyze and predict intermediate product performance is especially important. For instance, based upon a quality gate concept, a data-driven model was designed in [16] to diagnose the failure conditions and improve the control of battery manufacturing. Through using a data mining framework named the cross industry standard process, the neural network model was developed in [17] to predict and analyze the process dependency of battery production. Then, in [18], the conventional decision tree techniques were utilized to analyze the importance of intermediate variable and predict the maximal capacity of the manufactured battery. In [19], through using the recursive feature elimination solution, a data-driven approach was proposed to identify improvement potentials and analyze the relevant factors within the drying stage of battery manufacturing. After deriving a cyber-physical system based on quality gates, a data-driven model was proposed in [20] to predict future battery performance in battery manufacturing. In [21], after designing the multivariate process capability indices, a data-driven method was proposed to evaluate battery production data and achieve the quality assurance of the manufacturing process. In [22], after constructing the automatic relevance determination kernel from Gaussian process regression, parameters dependency within the mixing stage of battery production were evaluated.

Despite the aforementioned works through establishing the data-driven model for battery manufacturing, some limitations should be further improved. 1) The potential of extending the existing conventional methods toward more accurate prediction and better generality needs further evaluation; for example, as the battery electrode production is easy to generate lots of randomly distributed data, the class imbalance issue would frequently occur throughout the multiclass cases, which should be carefully considered. 2) Many works simply predict the battery product qualities via a commonly utilized machine learning technique (i.e., support vector machine and neural network) and fail to give reliable sensitivity analysis of feature variables within the battery production chain. It should be known that such analysis is also of specific interest to battery manufacturer as engineers could better understand the correlations of feature variables and their effects on the battery production chain, further benefiting the optimization and improvement of manufactured battery performance.

Given the aforementioned considerations, this article deals with the electrode quality classification during battery manufacturing via an ensemble learning approach, where the class imbalance issue is well solved and the sensitivity analysis of interested variables is directly conducted. Several main contributions can be made as follows. 1) After the identification of five key variables for electrode manufacturing, an ensemble

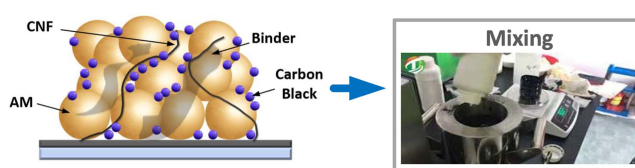


Fig. 1. Key components for electrode manufacturing.

learning based framework is developed to capture the underlying mechanisms among these variables and three key electrode qualities [electronic conductivity (EC), thickness, and capacity] of battery for the first time. 2) Through combining the benefits of both adaptive boosting (AdaBoost) and undersampling solution, a hybrid strategy named random undersampling boosting (RUBoost) is formulated to overcome the class imbalance issue and reduce the computational burden of electrode classification. 3) Two powerful evaluation metrics, the Gini importance and the predictive measure of association (PMOA), are derived within the RUBoost-based ensemble learning framework to simultaneously quantify the importance and correlations of battery formulation variables of interest. 4) The performance of the designed ensemble learning model is comprehensively analyzed for both experimental cases including LiFePO_4 (LFP) and $\text{Li}_4\text{Ti}_5\text{O}_{12}$ (LTO). Obviously, the designed model could accurately output the imbalanced class of battery electrode EC, thickness, and capacity. Moreover, the sensitivity analysis results provided by this RUBoost-based ensemble learning framework could be attributed back to the electrode manufacturing, further benefiting the control and optimization to achieve smarter battery production.

The rest of this article is organized as follows. Section II introduces the battery electrode production and the utilized data. The fundamentals behind the AdaBoost for multiclassification, RUBoost, and the framework to achieve electrode classification are then described in Section III. Section IV details the results and discussions with two case studies. Finally, Section V concludes this article.

II. ELECTRODE PRODUCTION AND EXPERIMENTAL DATA

Li-ion battery electrode production generally starts from a mixing stage, in which the prepared key formulation components would be mixed to generate slurries. Then the slurries would be coated onto the surface of current collector foils. Afterwards, the coating products are dried in ovens before they enter the calendaring stage [3]. The whole production chain contains the electrical, mechanical, and chemical disciplines, which must be carried out with specified equipment [18].

For the mixing stage, several components [i.e., active material (AM), electrode additive, and polymeric binder] would be mixed in a soft blender to generate slurry, as illustrated in Fig. 1. These component parameters must be carefully analyzed because they play the key and direct roles in determining the manufactured electrode qualities such as the EC and thickness, which would further affect the performance such as the capacity of battery products [4]. In reality, LFP and LTO are usually utilized as AMs. This is mainly because the LFP is nontoxic and highly adaptable

TABLE I
CLASS LABELS OF THE BATTERY ELECTRODE QUALITIES

Class labels	low	medium	high
EC (LFP)	≤ 15	(15, 20]	> 20
Thickness (LFP)	≤ 30	(30, 40]	> 40
Capacity (LFP)	≤ 120	(120, 135]	> 135
EC (LTO)	≤ 20	(20, 36]	> 36
Thickness (LTO)	≤ 30	(30, 40]	> 40
Capacity (LTO)	≤ 120	(120, 135]	> 135

to high temperature and large current, while LTO could mitigate the irreversible formation of solid electrolyte interphase and dendrite. In this context, manufactured batteries could present high power and long cyclic performance. Apart from them, electrode additives are also crucial for Li-ion batteries. Conductive fillers such as carbon black and carbon nanofiber (CNF) require to be added because the solo AMs' intrinsic EC would be insufficient. Besides, the polymeric binder is also important to give mechanical cohesion [4]. Due to the exceptional chemical stability and reliable binding property, three binder types including the polyvinylidene-fluoride (PVDF), polyethylene-co-ethylacrylate-co-maleic-anhydride (TPE), and hydrogenated-nitrile-butadiene-rubber (HNBR) are generally utilized [23].

In this article, based upon the experimental battery manufacturing data, an effective data-driven framework by using the ensemble learning technique is proposed to well classify and analyze the correlations among component parameters from mixing stages as well as their effects toward resulting the manufactured electrode product. Specifically, the components of interest contain two types of AMs (LFP and LTO), the carbon black with C65 grade, the CNF with 100 nm diameter, and three binder types including the PVDF with 14000 g/mol molecular weight, the HNBR dissolved within 99.5% purity N-methyl-pyrrolidone, and the TPE dissolved within 99.5% purity toluene. The qualities of interest include the thickness (μm) and EC (S/m) of electrode, and the capacity (mAh/g) of half-cell with C/25 charging and discharging rates under a temperature of 30 °C. Detailed ranges of each component with the weight fraction (%w) are as follows: The content of AMs varies from 75%w to 95%w; C65 varies from 0%w to 20%w; CNF is from 0%w to 10%w, while binder varies from 3%w to 20%w. Further explanations on the corresponding experiments and the effectiveness of this dataset can be found in [23]. The total numbers of data are 138 for LFP-based electrode and 108 for LTO-based electrode, respectively. Each observation is the average value of three experiments. To achieve the supervised learning process for our designed approach, predefined class labels are required. Following the same setting rules as some battery manufacturers, three class labels including low, medium, and high are set to reflect the manufactured electrode qualities [thickness, EC, and half-cell capacity] for both LFP and LTO runs.

Table I illustrates the class labels of battery production to classify all electrode qualities of interest. Fig. 2 shows the percentage of observations for all these electrode qualities. It is evident that there exists a large imbalanced percentage among each class. In comparison with the case of having the similar number of

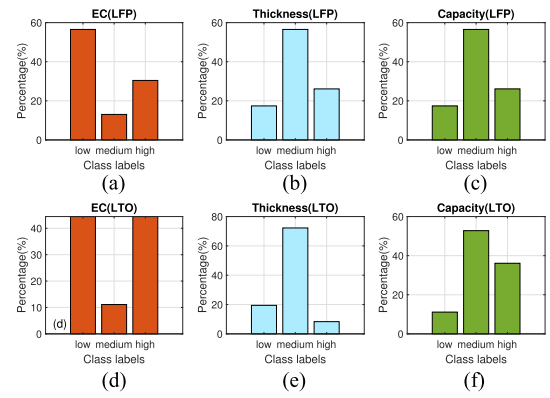


Fig. 2. Percentage of classified observations.

observations for each class label, this significantly different case results in a bigger challenge for classifications [24]. However, the class imbalance issue is easy to happen in battery electrode manufacturing process, which requires an effective solution to take this phenomenon into account.

III. METHODOLOGY

In this section, to design an ensemble learning based data-driven framework for achieving effective classification that considers the class imbalance issue, the fundamental of AdaBoost is first described. Then the RUBoost technique is elaborated, followed by the detailed presentations of designing the related data-driven framework.

A. Adaptive Boosting for Multiclassification

The class imbalance issue is easy to happen throughout the multiclassification cases. Because the misclassification would occur frequently for the minority classes, to derive an effective model in the case of various classes among experimental dataset being unevenly represented becomes challenging [25].

In general, two types of technologies including data sampling and boosting are utilized to alleviate the class imbalance issue [26]. For the data sampling strategy, the class observations within the training dataset would be balanced through adding samples to the minority classes (oversampling method) or reducing samples from the majority classes (undersampling method). It should be known that both oversampling and undersampling methods have merits and demerits. Specifically, undersampling could benefit the computational burden because the related training data size has been decreased. However, it would also cause some information loss associated with the deleted samples. Oversampling, on the contrary, would not lead to the information loss. But it could cause the overfitting and the increased computational burden.

Another effective strategy to overcome the class imbalance issues is the boosting technique in ensemble learning domain. In theory, boosting is able to enhance the classification performance of any weak learner no matter the defined classes are imbalanced or balanced. For the multiclass applications like the classifications of electrode qualities, one effective boosting

Workflow 1: Processes to Establish AdaBoost Ensemble Learning Model for Multiclassification

- 1: **procedure:** AdaBoost
- 2: Initializing the weights of training observations as: $W_i = 1/N, i = 1, 2, \dots, N$.
- 3: Supposing M is the number of all weak multiclass learners $L^{(j)}(X)$. For $j = 1$ to M :
 - a) Fitting a $L^{(j)}(X)$ to the training dataset based on the weights W_i .
 - b) Computing the $\text{err}^{(j)}$ as $\text{err}^{(j)} = \sum_{i=1}^N W_i \cdot I(L^{(j)}(X_i) \neq C_i) / \sum_{i=1}^N W_i$ where $I(\cdot)$ here represents the zero-one judgment with the rule of $I(L^{(j)}(X_i) \neq C_i) = 1$.
 - c) Computing the weight update factor $\alpha^{(j)}$ as $\alpha^{(j)} = \log[(1 - \text{err}^{(j)})/\text{err}^{(j)}] + \log(K - 1)$.
 - d) For $i = 1, 2, \dots, N$, updating the W_i as $W_i \leftarrow W_i \cdot \exp[\alpha^{(j)} \cdot I(L^{(j)}(X_i) \neq C_i)]$.
- e) Renormalizing W_i .
- 4: Outputting the predicted class $\tilde{C}(X)$ as $\tilde{C}(X) = \arg \max_k \sum_{j=1}^M \alpha^{(j)} \cdot I(L^{(j)}(X_i) = C_k)$ where C_k is the predefined class label ($k = 1 : K$), $I(L^{(j)}(X_i) = k) = 1$, $\arg \max_k$ outputs the class with the largest counting number from all weak learners.
- 5: **end procedure**

strategy is the AdaBoost [27]. Supposing a training dataset $\{(X_1, C_1), (X_2, C_2), \dots, (X_N, C_N)\}$ consists of N observations, X_i is a vector owing P variable terms of interest, C_i is the predefined class output with K class labels, and $L(X)$ represents a weak multiclass learner that outputs a class label related to X , then the detailed processes by establishing AdaBoost ensemble learning model for multiclassification could be summarized in Workflow 1.

B. Random Undersampling Boosting

In order to further improve the classification performance of electrode qualities with the issues of class imbalance, a hybrid strategy named random undersampling boosting is generated in this study based on the above-mentioned AdaBoost procedure. Workflow 2 details the processes to establish the related RUBoost-based ensemble learning model.

Obviously, one big difference between RUBoost and AdaBoost workflow is that in step 3 of each iteration, a random undersampling solution would be adopted for RUBoost to reduce the observations of the majority class until a desired percentage ($P\%$), further resulting in a new and temporary training dataset TD'_j . This TD'_j , therefore, has the new related weight distribution W'_j . Then the weak learner $L'^{(j)}(X)$ would be well trained based on both the TD'_j and W'_j . Through using this undersampling solution, RUBoost could not only give the balanced class observations for training but also reduce the related computational burden. On the other hand, although information loss may occur for a weak learner within the undersampling strategy, this lost information would be contained in establishing

Workflow 2: Processes to Establish RUBoost Ensemble Learning Model for Multiclassification

- 1: **procedure** RUBoost
- 2: Initializing the observation weights of all training dataset TD as: $W_i = 1/N, i = 1, 2, \dots, N$.
- 3: Supposing M is the number of all weak multiclass learners $L'^{(j)}(X)$. For $j = 1$ to M :
 - a) Creating a temporary training dataset TD'_j with related weights W'_j and percentage $P\%$ based on the random undersampling strategy.
 - b) Fitting a $L'^{(j)}(X)$ to the TD'_j based on W'_j .
 - c) Computing the $\text{err}^{(j)}$ based on the TD and W_i as $\text{err}^{(j)} = \sum_{i=1}^N W_i \cdot I(L'^{(j)}(X_i) \neq C_i) / \sum_{i=1}^N W_i$, where $I(L'^{(j)}(X_i) \neq C_i) = 1$.
 - d) Computing the weight update factor $\alpha^{(j)}$ as $\alpha^{(j)} = \log[(1 - \text{err}^{(j)})/\text{err}^{(j)}] + \log(K - 1)$.
 - e) For $i = 1, 2, \dots, N$, updating the W_i as $W_i \leftarrow W_i \cdot \exp[\alpha^{(j)} \cdot I(L'^{(j)}(X_i) \neq C_i)]$.
 - f) Renormalizing W_i .
- 4: Outputting the final predicted class $\tilde{C}(X)$ as $\tilde{C}(X) = \arg \max_k \sum_{j=1}^M \alpha^{(j)} \cdot I(L'^{(j)}(X_i) = C_k)$ where $I(L'^{(j)}(X_i) = k) = 1$.
- 5: **end procedure**

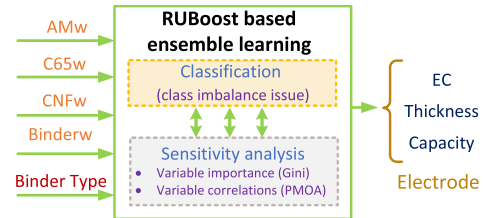


Fig. 3. Structure of RUBoost model for the electrode classification.

other weak learners [28]. In this context, the primary limitation of information loss within undersampling strategy could be significantly enhanced by the hybrid RUBoost solution.

C. Framework for the Electrode Classification

To well consider the class imbalance issue and analyze the sensitivity of interested material formulations in the electrode quality classification, a new RUBoost-based ensemble learning framework is designed in this study. Fig. 3 illustrates the structure of this ensemble learning model. Specifically, five variables including four material formulation contents [active material weight-fraction (AMw), C65 weight-fraction (C65 w), CNF weight-fraction (CNFw), and Binder weight-fraction (Binderw)] and Binder type are input into model to evaluate their effects on the classification performance of three battery electrode quality indicators (EC, thickness, and capacity). Detailed procedure of using this ensemble learning framework to quantify their correlations and to classify electrode qualities is summarized in Fig. 4 with four main steps as follows.

Step 1: Data curation and preprocess—the raw dataset would be first processed by removing the outliers and setting the class

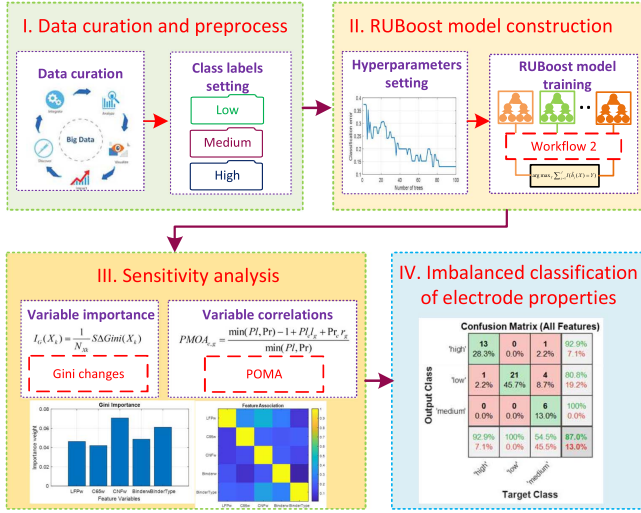


Fig. 4. RUBoost-based framework to conduct sensitivity analysis and classification for the battery electrode manufacturing.

labels. Following the defined setting rules in Table I, three quality indicators including the EC, thickness, and capacity are all classified with three class labels (low, medium, and high).

Step 2: RUBoost model construction—in this step, the hyperparameters require to be first set. The decision tree is generally utilized as the weak learner. Three main hyperparameters should be preset for the RUBoost-based ensemble learning model: the number of decision trees (M), the learning rate (r), and the desired percentage of entire samples to be represented by the minority class ($P\%$). For M , the classification accuracy could be enhanced through using more decision trees. However, too many decision trees would lead to the increased computational burden and overfitting problem. In our article, an iteration solution by evaluating the classification error is conducted to select suitable M . Second, r refers to the decay speed of the weight of each learner, while $P\%$ is utilized to balance class observations during training phase. As suggested in [29], setting r as 0.1 and $P\%$ as the percentage of minority class is a good solution. Afterwards, the RUBoost-based ensemble learning model would be well trained with the detailed procedure in Workflow 2.

Step 3: Sensitivity analysis—after well training the RUBoost-based model, the sensitivity analysis of variable importance and correlations could be carried out. On the one hand, through using the decision tree as a weak learner of ensemble learning, the variable importance could be effectively quantified by calculating the Gini importance of impurity variations caused by the splits on each variable item [30]. For multiclassification, impurity reflects how well the potential splits are for the nodes within the decision tree. The detailed procedure to calculate the Gini importance can be found in [30] for the readers of interest. A larger Gini importance value implies that the related variable item plays a more important role in determining the classification result. On the other hand, to quantify the correlations among different component parameters, the POMA is adopted. The general idea of getting POMA is to evaluate all potential splits with the optimal one which is observed in the training phase of

the decision tree. Let x_a and x_b represent two interested variable items ($a \neq b$), their POMA value could be calculated as

$$\text{POMA}_{a,b} = \frac{\min(Pl, Pr) - 1 + Pl_a l_b + Pr_a r_b}{\min(Pl, Pr)} \quad (1)$$

where l and r stand for the left and right children of node; Pl and Pr are the observation proportions of $x_a < u$ and $x_a \geq u$, respectively; $Pl_a l_b$ is the observation proportion under condition of $x_a < u$ and $x_b < v$, while $Pr_a r_b$ means the observation proportion under condition of $x_a \geq u$ and $x_b \geq v$. u and v , respectively, represent two values of variable item x_a and item x_b when the tree node is split into the left and the right parts during the process of tree generation. POMA is capable of reflecting the similarities between various decision rules to split observations. In this study, based upon (1), PMAOs of all variable item pairs are calculated and plotted with a form of 5×5 heat map.

Step 4: Imbalanced classification of electrode properties—after quantifying the formulation variable importance and correlations, the battery electrode qualities could be predicted and analyzed via the designed RUBoost model. In this article, to quantify and evaluate the classification result, the confusion matrix (CM) is utilized as the main performance indicator. Letting positive represent a class of interest while negative correspond to other classes, four basic metrics containing the true positive (TP), true negative (TN), false positive (FP), and false negative (FN) are first obtained. For the class (C_k) of interest (here $k = 1 : 3$), its precision rate ($\text{Prate}(C_k)$) and recall rate ($\text{Rrate}(C_k)$) are calculated to quantify the rate of all correct classification and all fraud cases as follows:

$$\begin{cases} \text{Prate}(C_k) = \text{TP}(C_k) / [\text{TP}(C_k) + \text{FP}(C_k)] \\ \text{Rrate}(C_k) = \text{TP}(C_k) / [\text{TP}(C_k) + \text{FN}(C_k)] \end{cases} \quad (2)$$

Then its F-measure ($\text{Fmeasure}(C_k)$) could be calculated to describe the harmonic mean of precision and recall as follows:

$$\text{Fmeasure}(C_k) = \frac{2 \times \text{Prate}(C_k) \times \text{Rrate}(C_k)}{\text{Prate}(C_k) + \text{Rrate}(C_k)} \quad (3)$$

A metric to reflect the accuracy of all multiclassifications named micro-F1 score (microF1) is obtained by

$$\text{microF1} = \frac{\text{TP}_{\text{all}} + \text{TN}_{\text{all}}}{N} \quad (4)$$

where $\text{TP}_{\text{all}} + \text{TN}_{\text{all}}$ means all correctly classified outputs and N is the total number of observations.

On the basis of the above-mentioned basic metrics, a CM with the form of 4×4 matrix is generated to effectively quantify the multiclassification results. For the CM, each row represents the predicted class, while each column is the actual class. The elements on the primary diagonal of CM reflect the correctly classified outputs while other elements are the incorrectly classified cases. The fourth row and column are the $\text{Rrate}(C_k)$ and $\text{Prate}(C_k)$ values of each class, respectively. The element in the final right-bottom corner is the microF1.

Based upon this procedure, a RUBoost-based ensemble learning framework is established to not only well classify the electrode qualities that have the imbalance class issue but also conduct effective sensitivity analysis for the variables of interest in Li-ion battery electrode formulation.

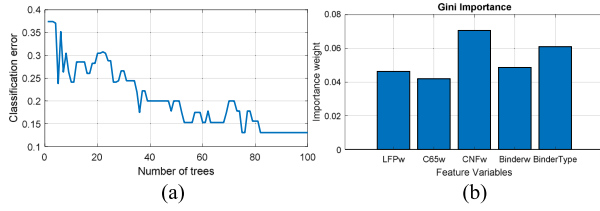


Fig. 5. Classification error and Gini importance for LFP EC case. (a) Classification error versus M . (b) Gini importance.

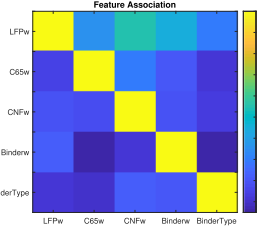


Fig. 6. Feature association for LFP EC classification case.

IV. RESULTS AND DISCUSSIONS

In this section, following all four steps from Section III-C, the tests by deriving suitable RUBoost based models are carried out to classify electrode quality indicators and to conduct sensitivity analysis of interested variables. For all case studies that use the RUBoost model, r is set as 0.1, while $P\%$ is set as the percentage of the minority class. An iteration solution by evaluating the classification error is conducted to select suitable M . Fivefold cross-validation is carried out for all the classification cases, leading to the training and test samples becoming 110 and 28 for LFP case studies and 86 and 22 for LTO case studies, respectively.

A. LFP Case Studies

We first consider a test for the LFP-based electrode to evaluate the effects of related AMw, C65 w, CNFw, Binderw, and Binder type on the multiclassification of electrode qualities. The performances of three classification cases (EC, thickness, and capacity) are all analyzed.

1) **Electronic Conductivity:** For the electrode EC, Fig. 5(a) illustrates the classification error versus the number (M) of decision trees. As M increases, the corresponding classification error would gradually reduce and converge to 0.13 after using 90 decision trees. Fig. 5(b) gives the quantified Gini importance for all formulation variables. It can be noticed that the Gini importance values of all these variables are larger than 0.04. The CNFw, Binder type, and LFPw are three most important variables to affect the classification results of electrode EC. Following (1), the heat map containing PMOAs of all variable pairs is obtained and plotted in Fig. 6. From this heat map, the largest PMOA appeared between LFPw and CNFw with 0.62, indicating these two variables have highest correlation for LFP-based EC classification case. Fig. 7(a) and (b) illustrates the related CMs by using all feature variables and just the three most important formulation variables (CNFw, Binder type, and

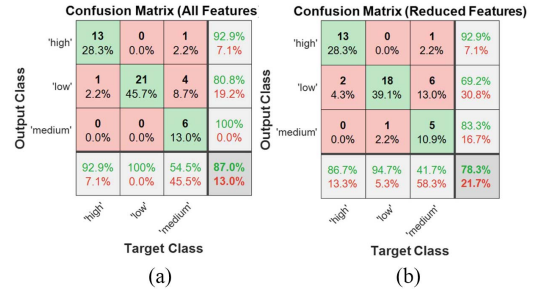


Fig. 7. Confusion matrix for LFP EC case. (a) All feature variables. (b) Reduced feature variables.

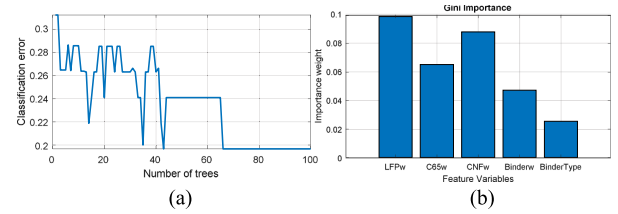


Fig. 8. Classification error and Gini importance for LFP thickness case. (a) Classification error versus M . (b) Gini importance.

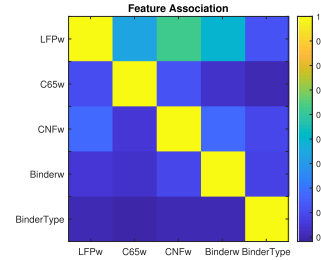


Fig. 9. Feature association for LFP thickness classification case.

LFPw), respectively. The microF1 of reduced-feature case is 78.3%, which is 10% less than that of all-feature case. This is reasonable as no significant difference exists here for the Gini importance weights of all component parameters.

2) **Thickness:** Based upon the RUBoost ensemble learning framework, the classification error versus M and the Gini importance of electrode thickness case are illustrated in Fig. 8(a) and (b), respectively. Obviously, the classification error converges to 0.19 after using 70 decision trees. The most important three variables for this case become LFPw, CNFw, and C65w, while the least important variable is Binder type. According to the corresponding heat map as shown in Fig. 9, the PMOA of LFPw and CNFw pair is larger than 0.55, indicating high correlation exists between this pair for LFP-based electrode thickness classification. Fig. 10 illustrates the corresponding CMs by using all feature variables and just three most important variables (LFPw, CNFw, and C65 w), respectively. The microF1 of reduced-feature case is 78.3%, which is only 2.6% less than that of all-feature case. This could also prove that the quantified variable importance is accurate.

3) **Capacity:** For the LFP-based electrode capacity case, the corresponding classification versus M and Gini importance are

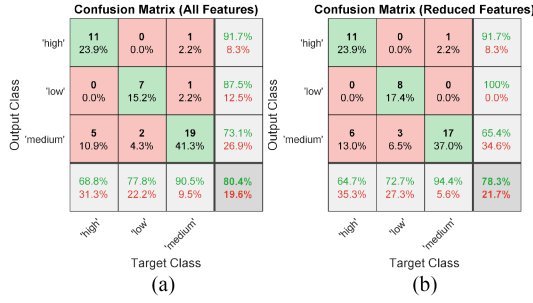


Fig. 10. Confusion matrix for LFP thickness case. (a) All feature variables. (b) Reduced feature variables.

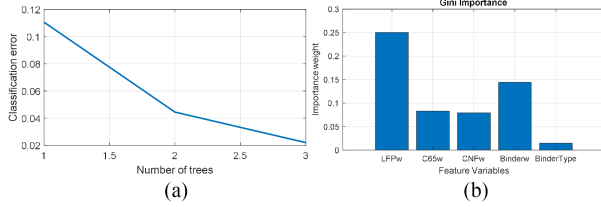


Fig. 11. Classification error and Gini importance for LFP capacity case. (a) Classification error versus M . (b) Gini importance.

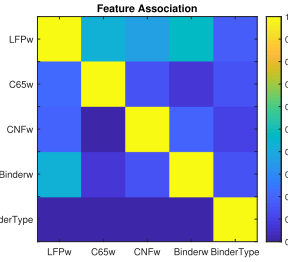


Fig. 12. Feature association for LFP capacity classification case.

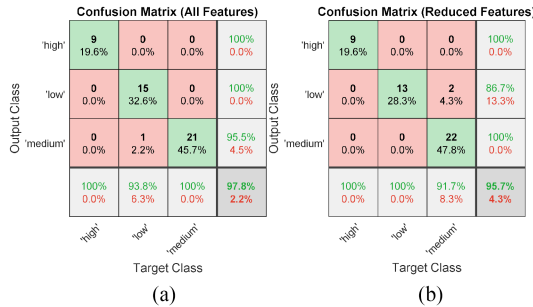


Fig. 13. Confusion matrix for LFP capacity case. (a) All feature variables. (b) Reduced feature variables.

illustrated in Fig. 11. Interestingly, the classification error for this case reduces to 0.02 after using just three decision trees, indicating that there should exist an approximate linear relation between these formulation variables and electrode capacity. The LFPw obtains the largest Gini importance weight, while C65w is a bit more important than the CNFw for this case. Besides, according to the heat map in Fig. 12, LFPw presents the relatively higher correlations with C65w, CNFw, and Binderw. Fig. 13 shows the CMs for the LFP electrode capacity case. The microF1

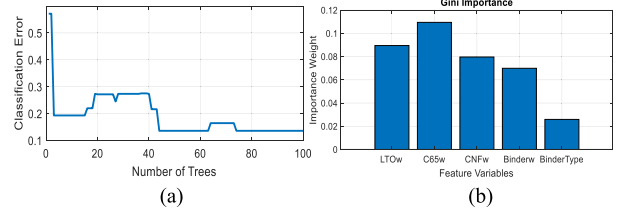


Fig. 14. Classification error and Gini importance for LTO EC case. (a) Classification error versus M . (b) Gini importance.

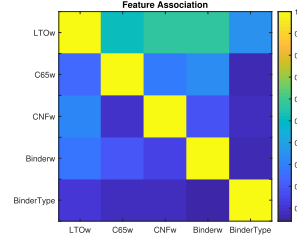


Fig. 15. Feature association for LTO EC classification case.

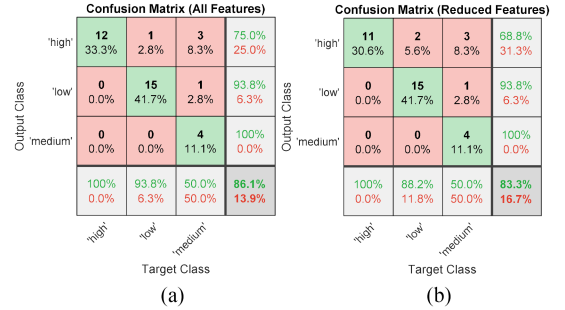


Fig. 16. Confusion matrix for LTO EC case. (a) All feature variables. (b) Reduced feature variables.

of both all-feature case and reduced-feature case reach 97.8% and 95.7%, respectively, which indicates the fantastic result can be obtained by using the proposed model to classify the LFP-based electrode capacity.

B. LTO Case Studies

Next, the test that uses the designed RUBoost-based framework to evaluate the effects of same component parameters on the multiclassification of battery electrode qualities is also carried out for LTO-based electrode.

1) *Electronic Conductivity*: Following the same procedures as LFP case, the classification error versus M and Gini importance for LTO-based electrode EC is shown in Fig. 14. In this case, the classification error converges to 0.14 after 76 decision trees are utilized. C65w, LTOw, and CNFw become the most three important component parameters. Based on the heat map in Fig. 15, the highest correlations existed for the pairs of LTOw and C65w. Fig. 16 illustrates the CMs of LTO-based electrode EC case. The microF1 of using the LTOw, Binderw, and C65w is 83.3%, which is 3.3% less than that of all feature variables. These results indicate that the effective classification results can be also achieved for LTO-based electrode EC case.

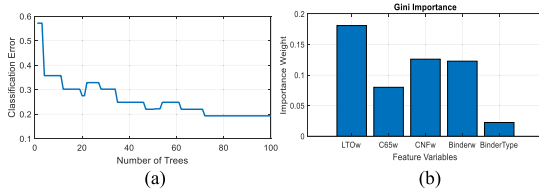


Fig. 17. Classification error and Gini importance for LTO thickness case. (a) Classification error versus M . (b) Gini importance.

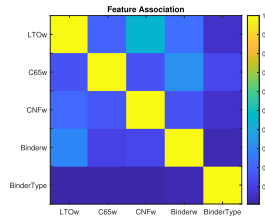


Fig. 18. Feature association for LTO thickness classification case.

Confusion Matrix (All Features)					Confusion Matrix (Reduced Features)				
Output Class	'high'	'low'	'medium'		Output Class	'high'	'low'	'medium'	
'high'	3 8.3%	0 0.0%	0 0.0%	100% 0.0%	'high'	3 8.3%	0 0.0%	0 0.0%	100% 0.0%
'low'	0 0.0%	7 19.4%	0 0.0%	100% 0.0%	'low'	0 0.0%	6 16.7%	1 2.8%	85.7% 14.3%
'medium'	6 16.7%	0 0.0%	20 55.6%	76.9% 23.1%	'medium'	5 13.9%	0 0.0%	21 58.3%	80.8% 19.2%
	33.3%	100%	100%	83.3%		37.5%	100%	95.5%	83.3%
	66.7%	0.0%	0.0%	16.7%		62.5%	0.0%	4.5%	16.7%
		'high'	'low'	'medium'			'high'	'low'	'medium'
		Target Class					Target Class		
		(a)					(b)		

Fig. 19. Confusion matrix for LTO thickness case. (a) All feature variables. (b) Reduced feature variables.

2) **Thickness:** Fig. 17 presents the classification error versus M and Gini importance of LTO-based electrode thickness. For this case, the classification error converges to 0.2 after using 73 decision trees. Apart from the Binder type, the Gini importance weights of all other formulation variables are larger than 0.06. The most important three items become LTOw, CNFw, and Binderw. According to the heat map in Fig. 18, three pairs including the LTOw and CNFw, C65w and Binderw, and Binderw and LTOw present the relatively higher correlations. According to the CMs in Fig. 19, it is interesting to note that although the specific classification results are different, both all-feature and reduced-feature cases achieve the same microF1 as 83.3%. It can be concluded that the component parameters of C65w, LTOw, and CNFw could almost determine the classification results of LTO-based electrode thickness.

3) **Capacity:** For the LTO-based electrode capacity case, the corresponding classification error converges to 0.06 after 92 decision trees are utilized, as illustrated in Fig. 20. The Binder type presents the lowest Gini importance value while LTOw, Binderw, and C65w lead to the three highest important weights that are all larger than 0.08. According to the heat map in Fig. 21, the pair of LTOw and CNFw achieves the highest PMOA, but its value is less than 0.5, indicating the correlations are small for this capacity classification case.

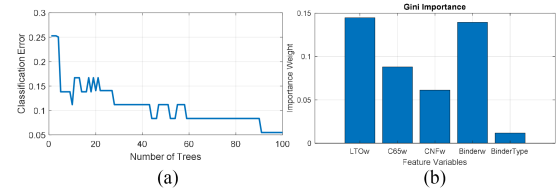


Fig. 20. Classification error and Gini importance for LTO capacity case. (a) Classification error versus M . (b) Gini importance.

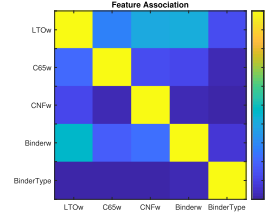


Fig. 21. Feature association for LTO capacity classification case.

Confusion Matrix (All Features)					Confusion Matrix (Reduced Features)				
Output Class	'high'	'low'	'medium'		Output Class	'high'	'low'	'medium'	
'high'	12 33.3%	0 0.0%	1 2.8%	92.3% 7.7%	'high'	12 33.3%	0 0.0%	1 2.8%	92.3% 7.7%
'low'	0 0.0%	4 11.1%	0 0.0%	100% 0.0%	'low'	0 0.0%	4 11.1%	0 0.0%	100% 0.0%
'medium'	0 0.0%	1 2.8%	18 50.0%	94.7% 5.3%	'medium'	0 0.0%	1 2.8%	18 50.0%	94.7% 5.3%
	100%	80.0%	94.7%	94.4%		100%	80.0%	94.7%	94.4%
	0.0%	20.0%	5.3%	5.6%		0.0%	20.0%	5.3%	5.6%
		'high'	'low'	'medium'			'high'	'low'	'medium'
		Target Class					Target Class		
		(a)					(b)		

Fig. 22. Confusion matrix for LTO capacity case. (a) All feature variables. (b) Reduced feature variables.

Interestingly, based upon the corresponding CMs in Fig. 22, the classification results of all-feature case and reduced-feature case are the same with both 94.4% microF1. This fact signifies that satisfactory classification can be achieved for LTO-based electrode capacity. On the other hand, the component parameters of LTOw, Binderw, and C65w are enough for accurately classifying the LTO-based electrode capacity.

C. Comparison and Discussion

1) **Comparison Studies:** To further verify the effectiveness of our proposed approach especially for handling the imbalanced class issue, another four popular tree-based ensemble machine learning approaches including the random forest (RF), AdaBoost, XGBoost, and LightGBM are utilized as the benchmarks for comparison purpose. To ensure a fair comparison, all these approaches are derived by using the MATLAB 2020 with a 2.40-GHz Intel Pentium 4 CPU. To be specific, RF adopts the bagging solution to generate weak learners [31]. Both XGBoost and LightGBM are based on the gradient boosting decision tree [32]. XGBoost decreases the overfitting issue through adding regular terms [33], while LightGBM adopts the leafwise strategy and uses the histogram to identify the optimal segmentation point [34]. Without the loss of generality, following the suggestions from [31] and [32], the number of weak learners for

TABLE II
COMPARISON RESULTS OF USING VARIOUS TREE-BASED ENSEMBLE
MACHINE LEARNING APPROACHES

LFP thickness			
Approaches	<i>microF1</i>	AUC	AET [s]
RF	75.1%	0.81	7.3
AdaBoost	75.3%	0.82	7.2
LightGBM	75.4%	0.82	6.9
XGBoost	76.7%	0.84	7.3
proposed method	80.4%	0.89	7.2
LTO thickness			
Approaches	<i>microF1</i>	AUC	AET [s]
RF	76.8%	0.87	6.8
AdaBoost	77.5%	0.89	6.8
LightGBM	77.8%	0.90	6.6
XGBoost	79.7%	0.91	6.9
proposed method	83.3%	0.94	6.8

all these ensemble machine learning approaches is set as 100. The number of features in each split of RF is fixed as 3. The learning rates of all other boosting-based approaches including the AdaBoost, XGBoost, LightGBM, and our designed RUBoost are all set as 0.1. To quantify the classification results of these approaches, three significant performance indicators including the *microF1*, the area under curve (AUC) of receiver operating characteristic, and the average execution time (AET) are adopted. After conducting fivefold cross-validation, the comparison results of using these tree-based ensemble machine learning approaches are illustrated in Table II, here the bold values indicate the best results. It can be noted that the AETs of all these approaches for both LFP thickness and LTO thickness cases are within 8 s, indicating that satisfactory computational effort can be achieved. RF presents the worst classification accuracy, while AdaBoost and LightGBM show similar classification accuracy. In comparison, our proposed method gives the best values of *microF1* and AUC for all cases (here, its *microF1* values are 4.8% and 4.5% higher than those from XGBoost, respectively). Therefore, our designed RUBoost approach presents competent performance to effectively handle the class imbalance issue for quality classification in battery electrode manufacturing.

2) Further Discussions: The RUBoost-based method proposed in this study has extensive application prospects for benefitting smarter and more automatic battery manufacturing. It is capable of effectively quantifying the importance weights of component parameters and the correlations of parameter pairs. Moreover, it could also well classify/predict the qualities of manufactured battery electrode considering the class imbalance issues. For the sensitivity analysis of component parameters, through using MATLAB 2020 with a 2.40-GHz Intel Pentium 4 CPU, the efficient calculation process can be achieved with a low computational burden of less than 10 s AET for all cases in this study. Then the proposed method is able to efficiently give the real-time classification/prediction of the electrode qualities after inputting a set of component parameters of interest. All these quantified or predicted information could help the battery manufacturer to better understand the manufacturing parameters of interest, distinguish the products with different quality levels at earlier stages, and readjust the component parameters to improve the manufactured electrode quality; further ensuring

the manufactured battery electrode can obtain satisfactory performance.

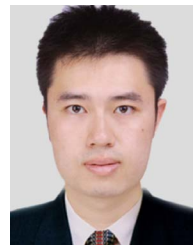
V. CONCLUSION

The class imbalance issue is easy to occur for the complicated battery electrode manufacturing and further affects the classification of related electrode qualities. In this article, a RUBoost-based ensemble learning framework is proposed to compensate for the class imbalance effect and achieve reliable sensitivity analysis in battery manufacturing chain. After experimental verification and comprehensive analysis for LFP- and LTO-based electrode production, some conclusions can be observed as follows. 1) The proposed ensemble learning framework shows to well handle the class imbalance issues and classify the electrode qualities accurately. 2) Based on the quantified Gini importance, the most important feature variables for all interested electrode qualities can be effectively discovered. Such information could not only help to simplify the model structure but also benefit the control and optimization of these feature variables. 3) The classification results for electrode capacities are significantly satisfactory with 97.8% accuracy for LFP and 94.4% for LTO, respectively. Besides, only three decision trees are utilized for the classification of LFP-based electrode capacity, indicating that there exists a strong linear relation for such case. The proposed ensemble learning framework presents the superiority in terms of accuracy, interpretability for both feature importance and correlations, data-driven nature, and the ability to handle the class imbalanced issue. When other battery manufacturing data such as the mixing speed, kneading intensity, temperature, and pressure from the mixing stage are available, it has a good potential in the reliable multiclassification and sensitivity analyses for these process parameters to benefit smarter battery manufacturing.

REFERENCES

- [1] H. Perez, N. Shahmohammadhamedani, and S. Moura, "Enhanced performance of li-ion batteries via modified reference governors and electrochemical models," *IEEE/ASME Trans. Mechatronics*, vol. 20, no. 4, pp. 1511–1520, Aug. 2015.
- [2] Y. Liu, R. Zhang, J. Wang, and Y. Wang, "Current and future lithium-ion battery manufacturing," *Science*, 2021, Art. no. 102332.
- [3] A. Kwade, W. Haselrieder, R. Leithoff, A. Modlinger, F. Dietrich, and K. Droeder, "Current status and challenges for automotive battery production technologies," *Nature Energy*, vol. 3, no. 4, pp. 290–300, 2018.
- [4] E. Kendrick, "Advancements in manufacturing," in *Future Lithium-Ion Batteries*, pp. 262–289, 2019.
- [5] Q. Tan, P. S. Divekar, Y. Tan, X. Chen, and M. Zheng, "Pressure sensor data-driven optimization of combustion phase in a diesel engine," *IEEE/ASME Trans. Mechatronics*, vol. 25, no. 2, pp. 694–704, Apr. 2020.
- [6] L. Wang, Z. Zhang, and X. Luo, "A two-stage data-driven approach for image-based wind turbine blade crack inspections," *IEEE/ASME Trans. Mechatronics*, vol. 24, no. 3, pp. 1271–1281, Jun. 2019.
- [7] X. Hu, Y. Che, X. Lin, and Z. Deng, "Health prognosis for electric vehicle battery packs: A data-driven approach," *IEEE/ASME Trans. Mechatronics*, vol. 25, no. 6, pp. 2622–2632, Dec. 2020.
- [8] K. Liu, X. Hu, Z. Wei, Y. Li, and Y. Jiang, "Modified gaussian process regression models for cyclic capacity prediction of lithium-ion batteries," *IEEE Trans. Transport. Electrification*, vol. 5, no. 4, pp. 1225–1236, Dec. 2019.
- [9] X. Hu, K. Zhang, K. Liu, X. Lin, S. Dey, and S. Onori, "Advanced fault diagnosis for lithium-ion battery systems," *IEEE Ind. Electron. Mag.*, vol. 14, no. 3, pp. 65–91, Sep. 2020.

- [10] K. Liu, K. Li, and C. Zhang, "Constrained generalized predictive control of battery charging process based on a coupled thermoelectric model," *J. Power Sources*, vol. 347, pp. 145–158, 2017.
- [11] C. Zou, C. Manzie, and D. Nešić, "Model predictive control for lithium-ion battery optimal charging," *IEEE/ASME Trans. Mechatronics*, vol. 23, no. 2, pp. 947–957, Apr. 2018.
- [12] K. Liu, C. Zou, K. Li, and T. Wik, "Charging pattern optimization for lithium-ion batteries with an electrothermal-aging model," *IEEE Trans. Ind. Inform.*, vol. 14, no. 12, pp. 5463–5474, Dec. 2018.
- [13] T. Liu, X. Hu, S. E. Li, and D. Cao, "Reinforcement learning optimized look-ahead energy management of a parallel hybrid electric vehicle," *IEEE/ASME Trans. Mechatronics*, vol. 22, no. 4, pp. 1497–1507, Aug. 2017.
- [14] J.-H. Schünemann, H. Dreger, H. Bockholt, and A. Kwade, "Smart electrode processing for battery cost reduction," *ECS Trans.*, vol. 73, no. 1, pp. 153–159, 2016.
- [15] T. Knoche, F. Surek, and G. Reinhart, "A process model for the electrolyte filling of lithium-ion batteries," *Procedia CIRP*, vol. 41, pp. 405–410, 2016.
- [16] J. Schnell and G. Reinhart, "Quality management for battery production: A quality gate concept," *Procedia CIRP*, vol. 57, pp. 568–573, 2016.
- [17] J. Schnell et al., "Data mining in lithium-ion battery cell production," *J. Power Sources*, vol. 413, pp. 360–366, 2019.
- [18] A. Turetskyy, S. Thiede, M. Thomitzek, N. von Drachenfels, T. Pape, and C. Herrmann, "Toward data-driven applications in lithium-ion battery cell manufacturing," *Energy Technol.*, 2019, Art. no. 1900136.
- [19] S. Thiede, A. Turetskyy, T. Loellhoeffel, A. Kwade, S. Kara, and C. Herrmann, "Machine learning approach for systematic analysis of energy efficiency potentials in manufacturing processes: A case of battery production," *CIRP Ann.*, vol. 69, no. 1, pp. 21–24, 2020.
- [20] A. Turetskyy, J. Wessel, C. Herrmann, and S. Thiede, "Data-driven cyber-physical system for quality gates in lithium-ion battery cell manufacturing," *Procedia CIRP*, vol. 93, pp. 168–173, 2020.
- [21] T. Kornas et al., "A multivariate KPI-based method for quality assurance in lithium-ion-battery production," *Procedia CIRP*, vol. 81, pp. 75–80, 2019.
- [22] K. Liu, Z. Wei, Z. Yang, and K. Li, "Mass load prediction for lithium-ion battery electrode clean production: A machine learning approach," *J. Cleaner Prod.*, 2020, Art. no. 125159.
- [23] O. Rynne et al., "Designs of experiments for beginners—a quick start guide for application to electrode formulation," *Batteries*, vol. 5, no. 4, p. 72, 2019.
- [24] A. Ali et al., "Classification with class imbalance problem: A review," *Int. J. Adv. Soft Comput. Appl.*, vol. 7, no. 3, pp. 176–204, 2015.
- [25] F. Thabtah, S. Hammoud, F. Kamalov, and A. Gonsalves, "Data imbalance in classification: Experimental evaluation," *Inform. Sci.*, vol. 513, pp. 429–441, 2020.
- [26] R. Longadge and S. Dongre, "Class imbalance problem in data mining review," 2013, *arXiv:1305.1707*.
- [27] C. Ying, M. Qi-Guang, L. Jia-Chen, and G. Lin, "Advance and prospects of adaboost algorithm," *Acta Automatica Sinica*, vol. 39, no. 6, pp. 745–758, 2013.
- [28] K. Liu, X. Hu, H. Zhou, L. Tong, D. Widanalage, and J. Marco, "Feature analyses and modelling of lithium-ion batteries manufacturing based on random forest classification," *IEEE/ASME Trans. Mechatronics*, to be published, 2021.
- [29] S. Mounce, K. Ellis, J. Edwards, V. Speight, N. Jakomis, and J. Boxall, "Ensemble decision tree models using rusboost for estimating risk of iron failure in drinking water distribution systems," *Water Resour. Manage.*, vol. 31, no. 5, pp. 1575–1589, 2017.
- [30] H. Liu and M. Cocea, "Induction of classification rules by Gini-index based rule generation," *Inf. Sci.*, vol. 436, pp. 227–246, 2018.
- [31] A. Cutler, D. R. Cutler, and J. R. Stevens, "Random forests," in *Ensemble Machine Learning*. Berlin, Germany: Springer, 2012, pp. 157–175.
- [32] W. Liang, S. Luo, G. Zhao, and H. Wu, "Predicting hard rock pillar stability using gbdt, xgboost, and lightgbm algorithms," *Math.*, vol. 8, no. 5, p. 765, 2020.
- [33] T. Chen and C. Guestrin, "XGboost: A scalable tree boosting system," in *Proc. 22nd ACM SIGKDD Int. Conf. Knowl. Discov. Data Mining*, 2016, pp. 785–794.
- [34] G. Ke et al., "Lightgbm: A highly efficient gradient boosting decision tree," *Adv. Neural Inform. Process. Syst.*, vol. 30, pp. 3146–3154, 2017.



management.



100 high-caliber journal/conference papers.



management of battery energy storage system.



includes power electronics, energy storage, and management systems. Dr. Guerrero is an Associate Editor for a number of the IEEE transactions.



Gothenburg, Sweden. His research interests include design and control of grid-connected converters for photovoltaic and wind power systems, and storage systems based on Li-ion battery applications including machine learning, modular converters, battery production, and active battery management systems.

Kailong Liu (Member, IEEE) received the Ph.D. degree in electrical engineering from Queen's University Belfast, Belfast, U.K., in 2018.

He is a Senior Research Fellow with the Warwick Manufacturing Group, University of Warwick, Coventry, U.K. He was a Visiting Student Researcher with the Tsinghua University, Beijing, China, in 2016. His research interests include modeling, optimization, and control with applications to electrical/hybrid vehicles, energy storage, battery manufacture, and

Xiaosong Hu (Senior Member, IEEE) received the Ph.D. degree in automotive engineering from Beijing Institute of Technology, Beijing, China, in 2012.

He is currently a Professor with the State Key Laboratory of Mechanical Transmissions and with the Department of Automotive Engineering, Chongqing University, Chongqing, China. His research interests include battery technologies and modeling and controls of electrified vehicles. He has authored or coauthored more than

Jinhao Meng (Member, IEEE) received the Ph.D. degree in electrical engineering from Northwestern Polytechnical University (NPU), Xi'an, China, in 2019.

He was supported by the China Scholarship Council as a joint Ph.D. student with the Department of Energy Technology, Aalborg University, Aalborg, Denmark. He is currently an Associate Researcher with Sichuan University, Chengdu, China. His research interests include battery modeling, battery states estimation, and energy

Josep M. Guerrero (Fellow, IEEE) received the Ph.D. degree in power electronics from the Technical University of Catalonia, Barcelona, Spain, in 2003.

Since 2011, he has been a Full Professor with the Department of Energy Technology, Aalborg University, Aalborg, Denmark, where he is responsible for the Microgrid Research Program. He has authored or coauthored more than 500 journal articles in the fields of renewable energy systems and microgrids. His research interests

Remus Teodorescu (Fellow, IEEE) received the Dipl.Ing. degree in electrical engineering from the Polytechnical University of Bucharest, Bucharest, Romania, in 1989, and the Ph.D. degree in power electronics from the University of Galati, Galati, Romania, in 1994.

In 1998, he joined the Power Electronics Section, Department of Energy Technology, Aalborg University, Aalborg, Denmark, where he is currently a Full Professor. Since 2013, he has been a Visiting Professor with Chalmers University, Gothenburg, Sweden. His research interests include design and control of grid-connected converters for photovoltaic and wind power systems, and storage systems based on Li-ion battery applications including machine learning, modular converters, battery production, and active battery management systems.